

Experimentation Lab, Physics 111B

Optical Pumping, OPT*

Sameen Yunus
Lab Partner: Gabe Otero
sfsyunus@berkeley.edu

02/20/2018

Abstract

The aim of this lab is to use the experimental method of optical pumping to verify the nuclear spins of Rb⁸⁵ and Rb⁸⁷, and to find the magnetic field strength of the earth in Berkeley. By applying a weak, uniform magnetic field we introduce energy level splittings in Rubidium atoms allowing us to optically pump them into a single excited state. Then by introducing a modulated radio frequency, we are able to de-excite the electrons in order to find the resonant frequencies for each isotope. Using the Breit-Rabi equation 01, our knowledge of Helmholtz coils 02, and our raw data, we are able to find a linear relationship between current and resonant frequency allowing us to calculate nuclear spins and field strength. We find the spins of Rb⁸⁵ and Rb⁸⁷ to be 5/2 and 3/2 respectively. And the strength of the magnetic field is found to be **0.2947 ± 0.00353 gauss**

Introduction

Optical pumping is a process developed by Nobel Prize winner, Alfred Kastler in the early 1950s. It allows atomic spectroscopy at radio frequencies to probe the smallest energy level splittings. This was previously not measurable due to thermal fluctuations at room temperature which provide enough energy to excite and de-excite electrons—the noise drowns out any spectroscopic information [1]. The method of optical pumping counters this by using circularly polarized light to align atomic spins in a given direction, thereby "pumping" all the electrons into a particular energy level and then using particular radio frequencies to de-excite these electrons [2]. In this experiment, we use optical pumping as a tool to measure the energy level splittings due to the Zeeman effect in Rubidium atoms placed in a magnetic field. Optical pumping is useful in our theoretical understanding of atomic physics as well in applications such as laser construction, atomic clocks and magnetometers.

*see Appendix A for signature sheet

Theory

To understand the theory of optical pumping, we need to delve into the quantum mechanical concepts of energy level splittings. In this experiment, we use a bulb filled with Rubidium gas made up of the isotopes ^{85}Rb and ^{87}Rb . Rubidium only has one valence electron which makes it easier to understand the pumping process and allows for simpler analysis.

Rubidium undergoes several natural energy level splittings starting with the Coulomb interaction between the electron and the nuclear charge. This is the largest energy difference splitting and in this case we care only about the outer most P and S shells. The Coulomb levels are further subdivided into fine structure levels which arise from spin-orbit interactions of the electrons. For the S state, there is only one sub-level while for the P state there exist 2 sub-levels with $J = \frac{3}{2}$ and $\frac{1}{2}$. J is the usual electron angular momentum: $J = S + L$ and combining this with the nuclear spins of the isotopes, I , we get the total angular momentum $F = J + I$. Beyond the fine structure splitting, each level is split again due to hyperfine splitting due to the nuclear magnetic dipole moment interacting with the magnetic spins of electrons which creates $2J$ more states. While we cannot interfere with splittings related to the atomic structure, a further splitting of the energy levels can be induced by applying an external magnetic field to the electrons known as Zeeman splitting. This splits each hyperfine level into $2F + 1$ levels quantized by the m_F quantum number. This structure is illustrated for ^{87}Rb in Figure 1 and the energy level diagram for ^{85}Rb varies as it has a different nuclear spin I which changes the F values and thus the Zeeman splitting is different [2].

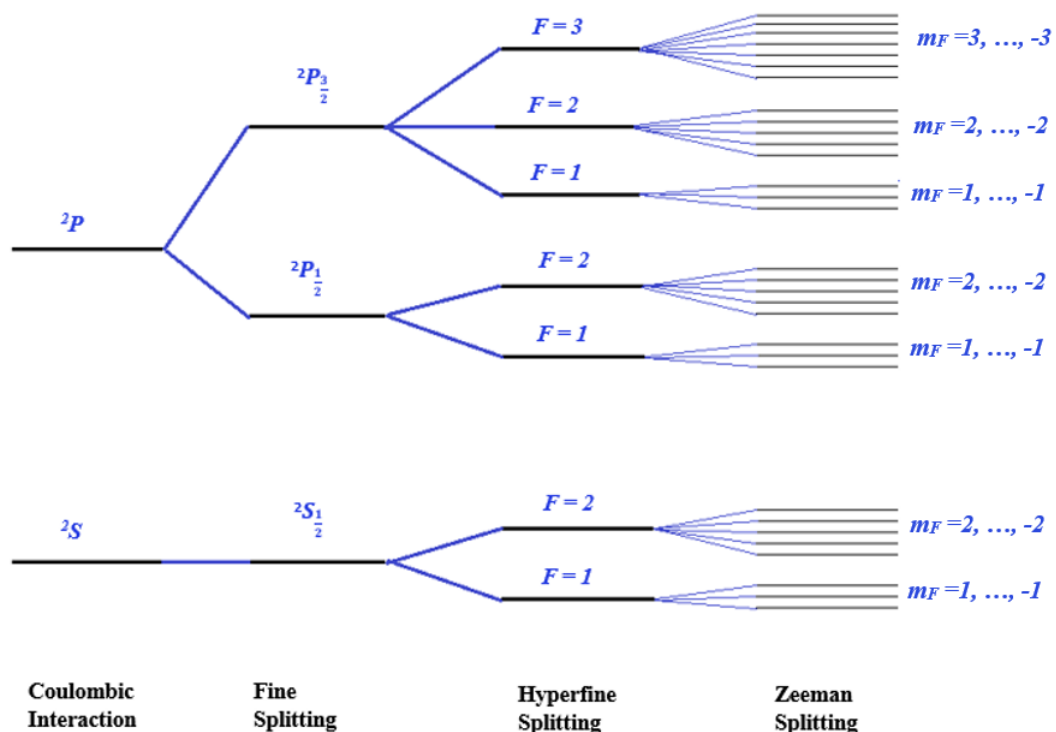


Figure 1: Atomic structure and Coulombic, fine structure, hyperfine structure, and Zeeman splittings for ^{87}Rb . Note that some of the $F = 1$ energy levels have a negative Lande g -factor which causes the m_F states to increase with lower energy.

Accounting for the Zeeman splitting energy difference in the Hamiltonian, we can arrive at the Breit-Rabi equation for the low field case [3] which relates the frequency of the electromagnetic waves to the total external magnetic field applied:

$$\frac{\nu}{B_{ext}} = \frac{2.799}{2I+1} \left(\frac{MHz}{Gauss} \right) \quad (01)$$

Here, I is the nuclear spin of the isotope which we will determine for ^{85}Rb and ^{87}Rb in this experiment along with the magnetic field of the earth.

The general principle of optical pumping is to pump electrons into a particular m_F state and then apply a specific radio frequency to de-excite them to a lower energy level. This can be achieved by sending in right circularly polarized light with a wide frequency range onto the bulb of Rubidium gas. The polarization of the light creates specific selection rules for the transitions where a photon is absorbed: $\Delta m_F = +1$ and $\Delta L = +1$ ¹. After some characteristic time, the electrons can spontaneously decay back to a lower energy level by the following selection rules: $\Delta m_F = 0, \pm 1$ and $\Delta L = \pm 1$. Once all of the electrons are pumped, we apply a radio frequency signal to make the electrons transition back down to a lower m_F state. Figure 2 illustrates these selection rules for two subsets of the $F = 1$ states. Suppose an electron starts in the $m_F = 0$ state in the $^2S_{1/2}$ level and transitions to the $m_F = 1$ state in the $^2P_{1/2}$ level. When losing a photon, the electron can either move to the $m_F = 0$ or the $m_F = 1$ state in the $^2S_{1/2}$ level. If it transitions to the the $m_F = 1$ state, its journey has come to an end since no further transitions are allowed. However if it comes down to the the $m_F = 0$ state the procedure will repeat until eventually all the electrons are pumped to the highest energy ground state manifold. The figure illustrates a small subset of the transitions, however they occur as allowed until eventually all the electrons are pumped into the $^2S_{1/2}, F = 3, m_F = +3$ state for ^{85}Rb and the $^2S_{1/2}, F = 2, m_F = +2$ state for ^{87}Rb .

As the Rubidium ions are being pumped, the light from the Rubidium lamp is being absorbed by the ions so the gas would appear opaque and we expect to see no signal from the photo-detector. However, as the ions become fully pumped, no more light is absorbed and all the optical signal from the lamp essentially passes through the gas and is collected at the detector. This is how we are able to detect whether or not pumping has occurred and what the resonant radio frequencies are.

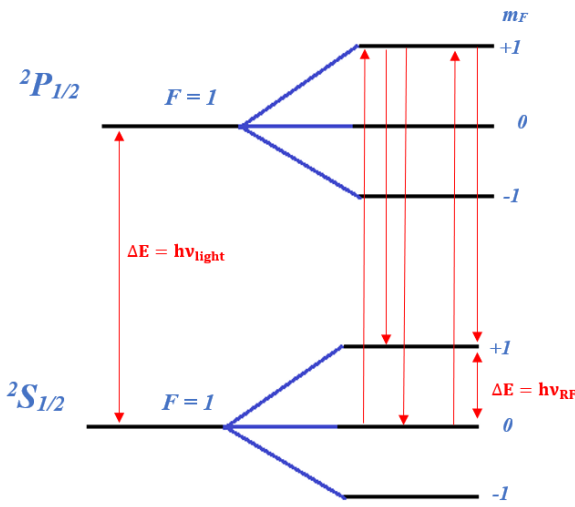


Figure 2: An example illustrating allowed transitions according to the selection rules for optical pumping for two subsets of $F = 1$ but all possible transitions will occur

As the Rubidium ions are being pumped, the light from the Rubidium lamp is being absorbed by the ions so the gas would appear opaque and we expect to see no signal from the photo-detector. However, as the ions become fully pumped, no more light is absorbed and all the optical signal from the lamp essentially passes through the gas and is collected at the detector. This is how we are able to detect whether or not pumping has occurred and what the resonant radio frequencies are.

¹The ΔL selection rule comes about because we limit our transitions to the lower energy member of the spin doublet: D1 [2]

Data and Apparatus

The experimental setup for optical pumping is quite straightforward as seen in Figure 3. Rubidium gas with 72% ^{85}Rb and 28% ^{87}Rb [2] is contained in a bulb (A). A Rubidium lamp (B) is used to shine light on the bulb with a circular polarizer that allows for our selection rules and filters out D2. There is a photo-detector (C) on the other side of the Rubidium cavity which measures the light passing through the gas and allows us to measure when the atoms have been pumped or de-pumped.

A heat control unit (D) modulates the temperature of heating coils in a box containing the bulb. However, having the heating coils turned on while taking measurements would introduce 60Hz noise therefore we had to turn on the heater to reach the desired temperature for each isotope and then turn it off when actually making measurements. The ideal temperature for ^{85}Rb is 30°C to 45°C and for ^{87}Rb is between 36°C and 48°C as these are the temperature ranges where the Rb gas stuck to the walls of the bulb gets vaporized and allows for a stronger optical signal.

The bulb is also wrapped with RF coils that are driven by the DS345 Signal Generator (E) to oscillate the radio frequency that will make electrons shift from the higher energy state. The entire apparatus

is enclosed by two Helmholtz coils (F) which, along with the earth's magnetic field, induce the Zeeman splitting that we study. The coils are aligned with the earth's field with an 11° measured angular offset with the coils turned on and off however, the field direction meter was behaving erratically so this measurement might be skewed. Regardless the error is small and contained within our measurement uncertainty so for the purposes of analysis we assumed the fields were perfectly aligned. Helmholtz coils produce a very uniform magnetic field in the space enclosed between the two coils where the field strength is measurable. Combining the magnetic field of the coils and of the earth (depending on the polarity of the coils) we can find the total magnetic field strength acting on the Rubidium cavity with:

$$B_{ext} = B_E \pm 0.9 \times 10^{-2} \frac{Ni}{a} \left(\frac{\text{gauss} \cdot \text{meter}}{\text{ampere}} \right) \quad (02)$$

Where B_E is the earth's magnetic field, N is the number of turns in the coil—135 for this experiment, i is the current in the coil, a is the radius of the coil—27.5cm for these coils. The coils can either be run with a DC power supply (G) or be modulated by a 60Hz sine wave in order to locate the resonant frequency. We will further explore these in the section of experimental methods.

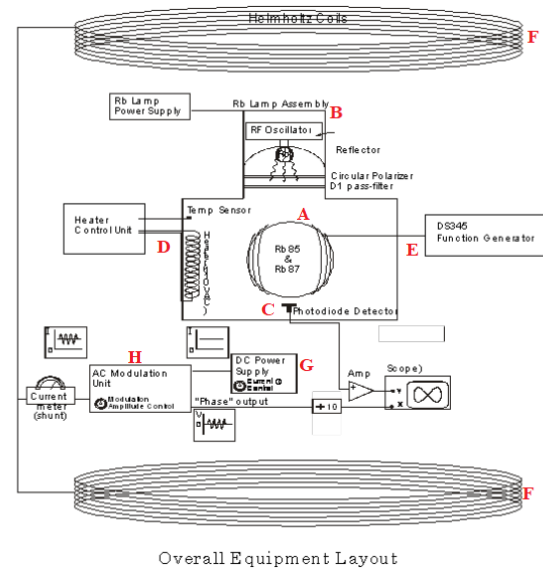


Figure 3: *Block diagram of optical pumping [3]. Labeled components are described in the text.*

Methods

Using the function generator to find resonance

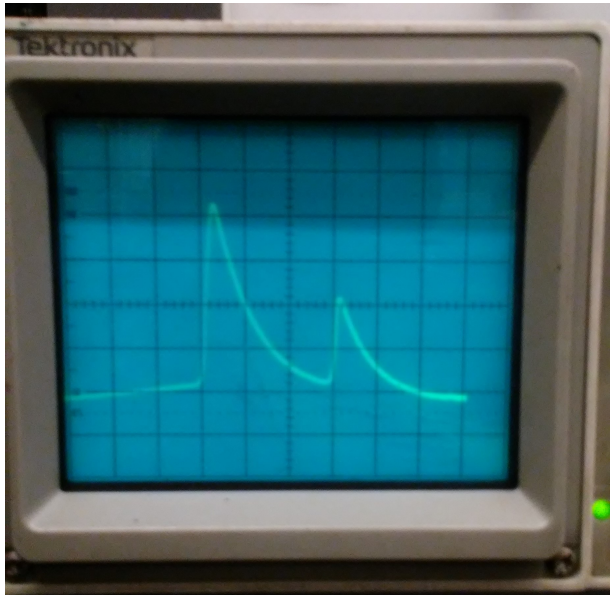


Figure 4: Trace on the oscilloscope screen with two peaks corresponding to the two resonant frequencies of the rubidium isotopes. The higher peak corresponds to the ^{85}Rb isotope and the shorter peak to the ^{87}Rb isotope. The x-axis reads the modulated frequency from the function generator and the y-axis is the readout from the photo-detector.

Since the resonant frequency depends only on the strength of the magnetic field, the measured resonance should not depend on the span of the function generator. However, it is difficult to narrow down the frequency range where resonance occurs accurately and as the peaks have variable width with time, we could only find the resonant frequency to within $\pm 200 \text{ kHz}$ which is not a reliable measurement. Therefore, we use the second method which involves modulating the magnetic field of the Helmholtz coils instead.

Using the coils to induce a modulating frequency to find resonance

While the previous method works as a quick check, a more reliable way is necessary in order to measure the values of resonant frequency within some reasonable error. To do so, we run some current through the Helmholtz coils and modulate this thereby changing the strength of the magnetic field instead of adjusting the RF. The coils should be modulated using 60 Hz line current and setting the modulation amplitude to about 30 mA . The phase output and photo-detector signals can then be displayed in the XY scope mode and if the apparatus is set up correctly, this should display a Lissajous figure as in Figure 5. The resonant frequency occurs when the Lissajous figure is most symmetric about the y-axis and the lobes are approximately the same size.

Assuming the magnetic field is held constant for any one value of the modulated current, as the RF is varied, we can understand why a symmetric Lissajous figure implies resonance. If the RF from the function generator is close to the resonant frequency for the magnetic field applied—then the strength of the magnetic field will oscillate around where the RF is resonant. In this case the time difference between the field reaching resonance oscillates between a short and long period which creates an asymmetric Lissajous figure. However, if the modulated field is close to the central field then the period between resonant strengths are equal and this results in a symmetric Lissajous figure. Hence, setting the RF to a value where the Lissajous figure becomes symmetric can demonstrate where the resonant frequency lies. There is of course, a range of frequencies over which we see a symmetric Lissajous figure, which accounts for systematic error in the measurement process that must be considered in analysis. Ideally, and as we will see in the next section, this error will be small and resonant frequencies can be measured quite accurately.

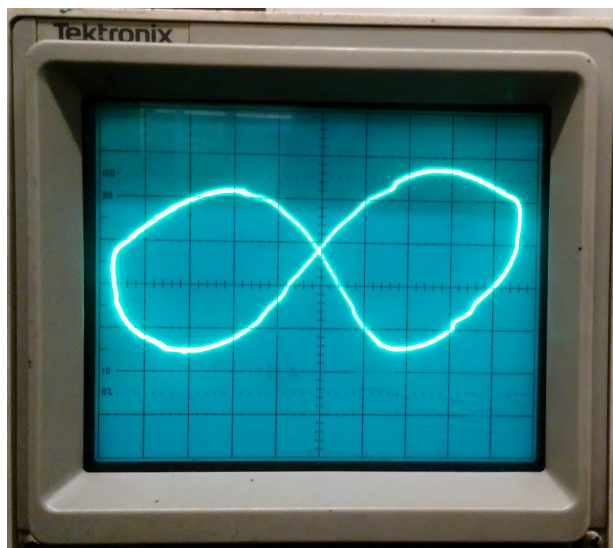


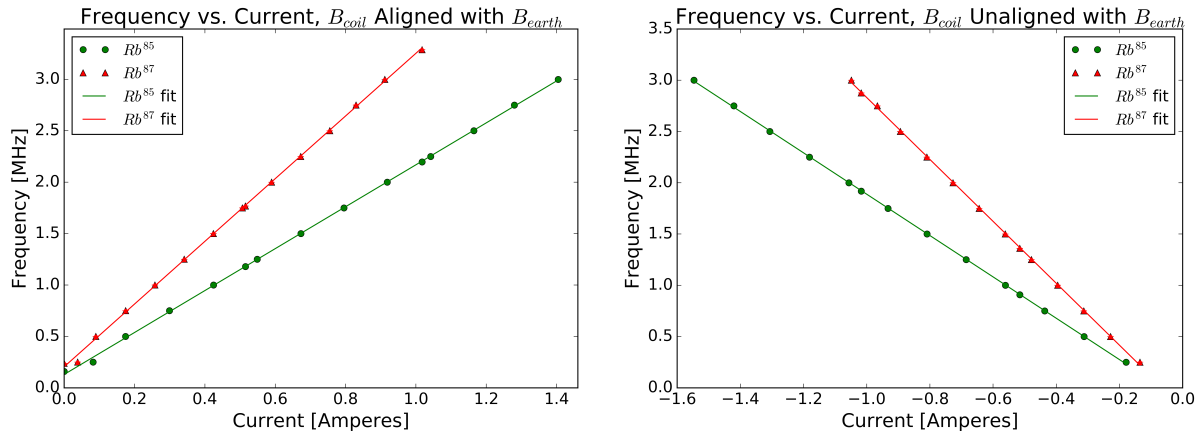
Figure 5: Oscilloscope screen showing a nearly symmetric Lissajous figure. The x-axis is the phase output of the magnetic field and the y-axis is the amplified photo-detector output. Since the figure is nearly symmetric, the magnetic field is near resonance.

Analysis

In order to acquire data we simply varied the current, i with the frequency, ν using the modulation of the Helmholtz coils to find resonant frequencies. For each value of ν we found two points, i where resonance occurred—these correspond to each of the two isotopes of Rubidium. We did this with the coil polarity on and off, meaning the direction of the magnetic fields from the Helmholtz coils was either in the same direction as the earth's magnetic field Figure 6a (polarity off) or in the opposite direction Figure 6b (polarity on). We can rearrange Equations 01 and 02 to get a linear relationship between ν and i :

$$\nu = \left(\frac{2.799}{2I+1} \frac{0.9 \times 10^{-2} N}{a} \right) i + \left(\frac{2.799}{2I+1} \right) B_E \quad (03)$$

We can assign negative values to frequencies for the coil polarity on configuration and plot all of our raw data as only two lines as in Figure 7 instead of four. Doing so will give us a better linear fit and as we will see further, a better approximation of B_E .



(a) ^{85}Rb and ^{87}Rb with coil polarity off. Error bars are plotted but too small to discern

(b) ^{85}Rb and ^{87}Rb with coil polarity on. Error bars are plotted but too small to discern.

Figure 6: Raw data and lines of best fit plotted for ^{85}Rb and ^{87}Rb with polarity on and off.

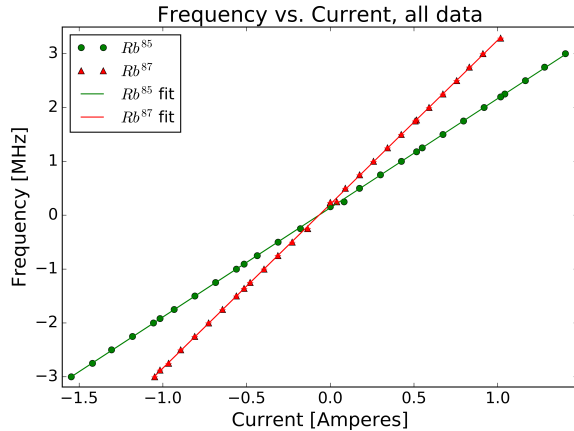


Figure 7: Data and line of best fit for both ^{85}Rb and ^{87}Rb showing all the data taken in both field orientations. The frequencies associated with negative currents are flipped about the x-axis to allow for a single fit. Error bars are plotted, but are too small to visually discern.

Before we can use our data to explore the behavior of the magnetic field and calculate the nuclear spins, I , we must first calculate the slopes, intercepts and errors of our best fit lines. To do so we can use the following equations 04 to find m and c using a conventional least squares method [5].

$$m = (\bar{iv} - \bar{i}\bar{v}) / (\bar{i^2} - \bar{i}^2) \quad c = \bar{v} - m\bar{i} \quad (04)$$

Where the notation \bar{i} and \bar{v} represents the statistical mean of our data. Furthermore, in order to find the errors in our fit we can use Equation 6.23 from Bevington [4]. We will later scale these errors by some constants to find I_1 , I_2 and B_E .

$$\sigma_m^2 = \frac{\sigma^2}{N \sum i^2 - \sum i^2} \quad \sigma_c^2 = \frac{\sigma^2 \sum i^2}{N \sum i^2 - \sum i^2} \quad \sigma^2 = \frac{1}{N} \sum (fit - data)^2 \quad (05)$$

Here σ^2 is the variance calculated from the residual errors and the errors in m and c follow from error propagation. Lastly we want to compute a goodness of fit statistic to ensure that our data is reliable, for linear regression we can determine the R^2 statistic, or the Coefficient of Determination which is the "*proportion of the variance in the dependent variable that is predictable from the independent variables*"[6] given by the following equation where the closer R^2 is to 1, the better your fit:

$$R^2 = 1 - \frac{\sum(fit - v)^2}{\sum(fit - \bar{v})^2} \quad (06)$$

We now have all the tools we need to conduct an analysis of the nuclear spins and magnetic field. The slopes, intercepts, errors and goodness of fit are summarized in Table 1

Isotope	m [MHz/A]	c [MHz]	σ_m [MHz/A]	σ_c [MHz]	R^2
^{85}Rb off	2.0390	0.1301	± 0.009420	± 0.007649	0.9996
^{85}Rb on	2.0164	0.1281	± 0.004730	± 0.004481	0.9999
^{85}Rb all	2.0280	0.1378	± 0.002793	± 0.002458	0.9999
^{87}Rb off	3.0486	0.2049	± 0.018806	± 0.010694	0.9994
^{87}Rb on	3.0192	0.1881	± 0.012079	± 0.008294	0.9997
^{87}Rb all	3.0446	0.2054	± 0.005768	± 0.003624	0.9998

Table 1: *Summary of slopes, intercepts, errors and goodness of fit for all of our data with both configurations of coil polarity and with the frequencies flipped along the x-axis.*

It should be noted that while recording data, there was a small read error in frequencies. This can be measured over the range of frequencies where the Lissajous figure appears to remain symmetric about the y-axis and we can attribute it to the sensitivity of the electronics. We measured the read noise in frequency to be around ± 800 Hz which is several order of magnitudes smaller than our statistical errors. We will later use this error to find the uncertainty in the zero-field resonance calculation of the earth's magnetic field.

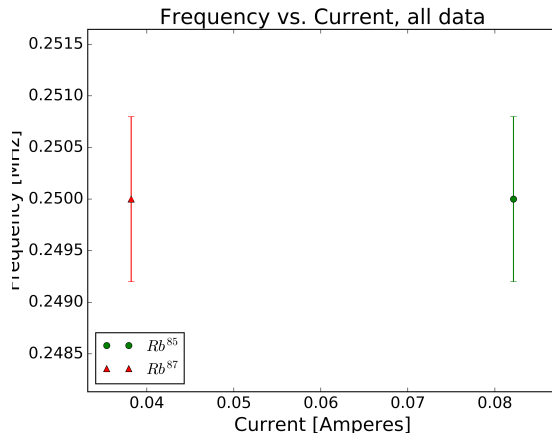


Figure 8: *Zoomed in error bars for raw data.*

Nuclear Spin

We explore two methods of finding I_1 and I_2 , where I_1 is the nuclear spin associated with ^{85}Rb and I_2 is for ^{87}Rb . From Equation 01 we can get a relation between ν_1 , I_1 and ν_2 , I_2 . If we select certain values of ν_1 and ν_2 from our data which are measured at the same value of current, and therefore the same external magnetic field, we can find a ratio ν_2/ν_1 which can tell us something about I_1 and I_2 .

$$\frac{\nu_2}{B_{ext}} = \frac{2.799}{2I_2 + 1} \quad \frac{\nu_1}{B_{ext}} = \frac{2.799}{2I_1 + 1} \quad \frac{\nu_2}{\nu_1} = \frac{2I_1 + 1}{2I_2 + 1} \quad (07)$$

Using our data points ² at a current value of 1.0174 A with the coil polarity turned off, we get:

$$\frac{\nu_2}{\nu_1} = \frac{3.2888}{2.1970} = 1.4969 \approx \frac{3}{2} \quad (08)$$

$$\frac{2I_1 + 1}{2I_2 + 1} = \frac{3}{2} \quad 3I_2 + \frac{3}{2} = 2I_1 + 1 \quad 2I_1 - 3I_2 = \frac{1}{2} \quad (09)$$

We are able to round to $3/2$ because we know that both the nuclear spins are half integer. Then from the last equation in 09 we can deduce that $\mathbf{I}_1 = 5/2$ and $\mathbf{I}_2 = 3/2$.

Another way of determining the spins is to rearrange the Breit-Rabi equation 01 and the equation for the magnetic field of the Helmholtz coils 02. Note that we can also derive the same equation from the slope of our best fit lines. We use these slopes and propagate the errors to fine I_1 and I_2 .

$$m = \frac{2.799}{2I+1} \frac{0.9 \times 10^{-2} N}{a} \quad I = \frac{1}{2} \left(\frac{2.799 \cdot 0.9 \times 10^{-2} \cdot N}{m \cdot a} - 1 \right) \quad (010)$$

Also from our knowledge of error propagation³, we know

$$\text{For } R = R(X) \quad \sigma_R^2 = \left(\frac{\partial R}{\partial X} \right)^2 \sigma_X^2 \quad (011)$$

$$\sigma_I^2 = \left(\frac{\partial}{\partial m} \left(\frac{\alpha}{m} + \frac{1}{2} \right) \sigma_m \right)^2 \quad \sigma_I^2 = \left(\frac{-\alpha}{m^2} \sigma_m \right)^2 \quad \alpha = \frac{2.799 \cdot 0.9 \times 10^{-2} \cdot N}{a} \quad (012)$$

Finally, we can use the above series of equations and Table 1 to find the values of nuclear spins for all our data and the associated errors in Table 2. We expect ^{85}Rb to have $I_1 = 5/2$ and ^{87}Rb to have $I_2 = 3/2$. The computed values are close and we can round them to half integers but they are not exact, even after accounting for errors. This may be because for this calculation we neglect the magnetic field of the earth as $B_{ext} = B_{coil} \pm B_E$ however, here we are considering only B_{coil} .

²see Appendix C

³Refer to page 43 Hughes and Hase [7]

Isotope	I	σ_I
^{85}Rb off	2.5324	± 0.02801
^{85}Rb on	2.5663	± 0.01438
^{85}Rb all	2.5488	± 0.00839
^{87}Rb off	1.5281	± 0.02502
^{87}Rb on	1.5479	± 0.01638
^{87}Rb all	1.5308	± 0.00769

Table 2: Computed values of I_1 and I_2 using the slopes and errors found from our data. If we round to half integers. the values agree with the expected $I_1 = 5/2$ and $I_2 = 3/2$.

Earth's Magnetic Field

Since we now know I_1 and I_2 , we can go on to compute B_E using various methods such as the intercepts of the best fit lines, the zero field method and the negative current values method.

Using the intercepts of best fit lines to find B_E

Starting with the y-intercepts of the best fit lines, we can find B_E as when the current is 0 A, the only magnetic field acting on the Rubidium is that of the earth. We can use the following equations to find B_E and the error from the fit as summarized in Table 3:

$$c = \left(\frac{2.799}{2I+1} \right) B_E \quad B_E = \frac{2I+1}{2.799} c \quad \sigma_{B_E}^2 = \left(\frac{2I+1}{2.799} \sigma_c \right)^2 \quad (013)$$

Isotope	I	B_E	σ_{B_E}
^{85}Rb off	5/2	0.2789	± 0.01639
^{85}Rb on	5/2	0.2746	± 0.00960
^{85}Rb all	5/2	0.2955	± 0.00526
^{87}Rb off	3/2	0.2929	± 0.01528
^{87}Rb on	3/2	0.2688	± 0.01185
^{87}Rb all	3/2	0.2936	± 0.00517

Table 3: Computed values of B_E and the associated errors using using the intercepts and errors found from our data, and from knowing what I_1 and I_2 are from the previous section. Fields are measured in [gauss]

The values of B_E calculated from the individual data sets for each isotope and polarity configuration separately are not reliable values as they fall outside of the statistical errors for each other. The value for the intercept calculated for each isotope with the polarity configurations combined is more reliable since we use more data to fit that line—concurrently the values of B_E computed from these intercepts are more accurate and they both fall within the errors for each other.

Using positive and negative current values to find B_E

However, there is a more effective way to calculate the earth's field. The total magnetic field acting on the Rubidium bulb is:

$$B_{ext} = B_{coil} \pm B_E$$

Thus, if for every positive current data point a corresponding negative current data point with the same absolute value of current is taken, then plugging in the data to the Breit-Rabi equation 01 and adding the two resulting equations would result in a formula containing only resonant frequencies, earth's magnetic field, and constants as follows:

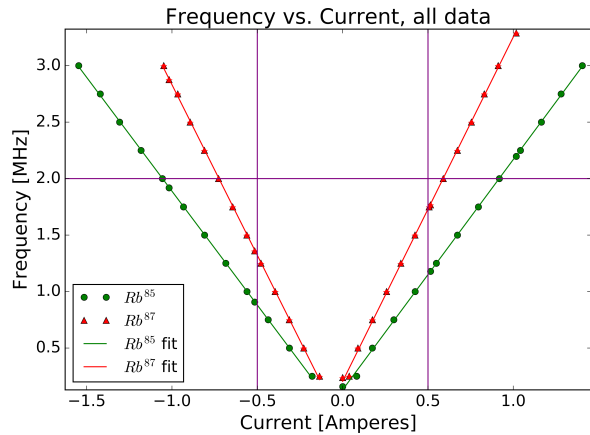


Figure 9: Parallel and vertical lines to extrapolate values.

$$\nu^+ = \frac{2.799}{2I+1} |B_{coil}| + |B_E| \quad \nu^- = \frac{2.799}{2I+1} |B_{coil}| - |B_E| \quad (014)$$

$$B_E = \frac{1}{2} \left(\frac{2I+1}{2.799} \right) |\nu^+ - \nu^-| \quad (015)$$

We computed B_E using two absolute current values and the error was found using the 800 Hz read noise in the DMM as discussed previously. We can see that these values are within the given errors and also within the errors of the reliable values from the previous method.

Figure 9 shows two vertical lines at $i = \pm 0.5$ A. This can be used to extrapolate the negative and positive frequency values used to find the values of B_E in the table above. We used values around 1 A from our data however using this method we can evaluate the expected frequencies at any point on the curve.

Isotope	i_{\pm} [A]	ν_+ [MHz]	ν_- [MHz]	I	B_E	σ_{B_E}
^{85}Rb	1.0174	2.197	1.9182	5/2	0.2988	± 0.0012126
^{85}Rb	0.5153	1.179	0.9074	5/2	0.2916	± 0.0012126
^{87}Rb	1.0174	3.288	2.8759	3/2	0.2950	± 0.0008084
^{87}Rb	0.5153	1.768	1.3600	3/2	0.2915	± 0.0008084

Table 4: B_E evaluated using the negative currents method. Fields are measured in [gauss]

Using the Helmholtz coil equation to find B_E ⁴

Once again, using positive and negative values of current, we can find B_{ext} from the Breit-Rabi equation.

$$B_{ext+} = \frac{2I+1}{2.799} \nu^+ = \frac{2I+1}{2.799} \nu^+ \quad B_{ext-} = \frac{2I+1}{2.799} \nu^- \quad (016)$$

⁴This section corresponds to "Problem 3" in the analysis section of the lab writeup.

Now, if we compare these values with that found using the Helmholtz coil equation 02, there will be an obvious discrepancy because B_E is not accounted for. However, if we note that,

$$B_{ext+} = B_{coil,1} + B_E \quad B_{ext-} = B_{coil,1} - B_E \quad B_E = \frac{1}{2}(B_{ext+} - B_{ext-}) \quad (017)$$

Then we can another set of values for B_E in addition to finding a more accurate value for B_{coil} in comparison to the value from equation 02. This assumes that the radius of the coil is even for each of the N turns and that is not necessarily true. Instead, we can find a more accurate value using $B_{coil,2} = B_{ext} \pm B_E$.

Isotope	$i[A]$	$v[MHz]$	B_{ext}	$B_{coil,1}$	B_E	σ_{B_E}	$B_{coil,2}$	$\sigma_{B_{coil}}$
^{85}Rb	1.0174	3.2888	4.6999	4.4952	0.2950	± 0.00121	4.4049	± 0.046
^{85}Rb	-1.017	2.8759	4.1098					
^{87}Rb	1.0174	2.1970	4.7095	4.4952	0.2988	± 0.0008084	4.4107	± 0.042
^{87}Rb	-1.017	1.9182	4.1118					

Table 5: Summary of the magnetic fields of the coil and the earth based on the equations above. $B_{coil,1}$ is the value from Equation 02, while $B_{coil,2}$ is the more accurate value found from knowing B_E . Fields are measured in [gauss]

Zero field

The zero field resonance occurs when we cancel out the magnetic field of the earth with that of the coil and a total $B_{ext} = 0$ is acting on the Rubidium bulb. In order to do this, we turn off the frequency modulation and simply locate the value of current for the Helmholtz coils where we see a symmetric Lissajous figure. Physically, once the magnetic field is removed, the m_F states become degenerate and as there is no longer any distinction between them they are free to switch between the energy levels therefore we see resonance even in an unpumped state.

We found that the zero field instance occurs when we run a current of -0.06069 A through the coils. We can use the Helmholtz coils equation 02 as this translates essentially to a current of $+0.06069\text{ A}$ corresponding to the field of the earth. Then using $N = 135\text{ turns}$ and $a = 27.5\text{ cm}$, we find $B_E = 0.2681 \pm 0.002$. This is far outside of the range of acceptable values from our accurate measures of B_E as there is a much larger error introduced by the inaccuracy of the equation in assuming N and a are constant. In addition, there is also a read error introduced by the "cancellation" of the fields which is accounted for in the error listed above.

What is the best value of B_E ?

After exploring several methods of computing B_E we find that the most accurate values are given by the negative and positive equal currents method, and by the slope of the best fit line using all the available data. Hence, we can perform a weighted average of the values and find a nominal value of $B_E = 0.2947 \pm 0.00353\text{ gauss}$

Measuring the pumping and relaxation time

To get an understanding of the physical timescales we are working with, we can experimentally determine a rough estimate of the time it takes all the atoms to be fully pumped and then the time it takes for them to relax to a lower energy level. To do so, we modulate the RF with a square wave and a low rate of modulation, the gas will reach equilibrium before the RF changes amplitude and we will be able to measure the finite pumping and relaxation time of Rubidium. One e-folding, or the time it takes the signal to change by $1/e$ corresponds to the characteristic time scale. Doing so we found roughly **$t_{\text{pump}} = 25 \text{ ms}$** and **$t_{\text{relax}} = 70 \text{ ms}$** .

In order to compare this to a theoretical value of these times we would need to know the concentration and volume of Rubidium to other isotopes in the bulb. The more Rubidium there is, the longer it would take to be fully pumped. And this must also account for the Rubidium stuck to the walls and how much of it vaporizes at what temperatures. To compute the relaxation time, we need to know the temperature of the bulb and whether or not the bulb is coated in parafin wax—this keeps the Rubidium atoms from hitting the glass walls and retaining their spin polarization and they stay pumped for longer.

Additional sources of error

In this section we review a few of the sources of error that were not accounted for in analysis. Firstly, we studied the temperature dependence of the optical signal in the range of optimum temperatures for both isotopes of Rubidium. We found that over a range of $\Delta T \approx 20^\circ$ the signal changed by 3.5 A for ^{85}Rb and by 5.3 mA for ^{87}Rb . Additionally, for each measurement of resonant frequency, we found a read error of approximately $\pm 5\text{mA}$ in the current. The temperature dependence and the read error are both orders of magnitude smaller than our statistical errors therefore we neglected to include them in analysis. In addition, our measurement of the field alignment was likely skewed—we measured the coils to be 11° out of alignment with B_E using the field direction meter. We disregarded this error however, small as it is, the angular shift introduces some angular components to the equations governing B_{ext} , B_{coil} and B_E which was not considered.

Conclusion

By using an oscillating magnetic field generated by Helmholtz coils that were aligned with the Earth's magnetic field, a Rubidium lamp with a D1 pass filter, and a circular polarizer, we were able to optically pump a cavity full of Rubidium gas by creating Zeeman splitting energy levels. Using several different techniques we were able to calculate and verify the strength of earth's magnetic field. In addition, we were able to use the Breit-Rabi equation and a line of best fit with our data to identify the nuclear spins of the two isotopes of Rubidium. Our results showed the spins of ^{85}Rb and ^{87}Rb are $5/2$ and $3/2$ respectively. In addition, we found the earth's magnetic field to be $0.2947 \pm 0.00353 \text{ gauss}$. These values are within a reasonable error of the values quoted by the National Centers for Environmental Information[8].

References

- [1] A.L. Bloom, *Optical Pumping*, Scientific American, October 1960, p.72.
- [2] R.L. De Zafra, *Optical Pumping*, Amer. Journ. of Phys. 28, 646 (1960)
- [3] D. Orlando. Optical pumping, 2018. <http://labs.physics.berkeley.edu/mediawiki/index.php/OpticalPumping>
- [4] Bevington, P., *Data Reduction and Error Analysis for the Physical Sciences*. McGraw-Hill
- [5] Graham, J., R., *Conventional Linear Least-Squares Fitting* <https://drive.google.com/file/d/0B40Ynk22SiBpSU1DN2dPN3pzNXc/view>
- [6] Coefficient of determination, https://en.wikipedia.org/wiki/Coefficient_of_determination
- [7] Hughes, I. G. and Hase, T. P. A., *Measurements and their Uncertainties, A Practical Guide to Modern Error Analysis*. Oxford University Press, 2010
- [8] National Centers for Environmental Information, National Oceanic and Atmospheric Administration, <https://www.ngdc.noaa.gov/geomag-web/#igrfwmm>

Appendix A

Signature Sheet

OPT - Optical Pumping
Signature Sheet

Student's Name Sameen Yunus Partner's Name Gabe Otero

Pre-Lab Discussion Questions

It is your responsibility to discuss this lab with an instructor before your first day of your scheduled lab period. This signed sheet must be included as the first page of your report. Without it you will lose grade points. You should be prepared to discuss at least the following before you come to lab:

- What is the general principle of optical pumping? Go over your derivation of the Breit-Rabi formula and the values of the Lande g-factors of the hyperfine energy levels of ^{85}Rb and ^{87}Rb . Draw qualitative energy-level diagrams for ^{85}Rb and ^{87}Rb showing the fine, hyperfine, and Zeeman splittings. How do the Lande g-factors affect the ordering of the Zeeman levels? Show the transitions between these levels that are important to this experiment. Include these drawings in your write-up. For our rubidium system, what is the pumping process? Where is the pumped level? Where is the RF transition?
- Why do we modulate (very sinusoidally) the external magnetic field? How would we take data if the magnetic field were not modulated?
- In this experiment, how will you determine the resonance frequency? How can you best estimate the error? Will the modulation amplitude affect your result? What data will you take, and what plots will you make?

Staff Signature Bhattacharyya Date 1/29/18

Completed before the first day of lab? (Circle one) Yes No

Mid-Lab Discussion Questions

- On day 2 of this lab, you should have successfully produced a plot of frequency versus current for at least one rubidium isotope, and have made an estimate of the earth's magnetic field. Show them to an instructor and ask for a signature.

Staff Signature Bhattacharyya Date 1/30/18

Completed by day 2 of lab? (Circle one) Yes No

1

Checkpoint Signatures

1. DS345 Preparation

Staff Signature [Signature]

2. Resonance Conditions and Symmetry

Staff Signature Bhattacharyya

3. Error Analysis Methods

Staff Signature lu lu

Appendix B

Pre-lab

Problem 1

** Note: the energy level diagrams are included in the write up. The derivation of the Breit-Rabi equation was discussed at length with a GSI and is very long to type up. And we were told in the write up not to include our calculation of the Lande-g factors as this is also a lengthy but obvious calculation.**

Optical pumping involves sending polarized light with a wide energy (frequency) range into an atom and allowing for the electrons to transition to higher energy levels. They will spontaneously decay down to the highest energy ground state manifold level because of the selection rules based on the polarization of the light. We can then propagate RF waves into the medium and at some specified frequency, which matches the Zeeman splitting energy levels, (in this case) the electrons will be de-excited and the optical signal will reflect this based on the intensity of the signal passing through the medium.

For our system, the pumping process is to

- Turn on equipment and electronics. Turn on the magnetic field to "create" the Zeeman splitting
- Circularly polarized light is shined on the bulb
- We then wait to see a high optical signal which indicates that the electrons are in the pumped state and no more photons are absorbed.

The pumped state is $^2S_{1/2}$, $F = 3$, $m_F = +3$ state for ^{85}Rb and the $^2S_{1/2}$, $F = 2$, $m_F = +2$ state for ^{87}Rb . And the RF transition occurs between the pumped state and the $m_F = 0$ ground state.

Problem 2

The sinusoidal oscillations around resonance allow us to more clearly determine where the resonance frequency is because that produces a Lissajous figure. The detector output oscillates in time at resonance. If we aren't modulating the magnetic field with the Helmholtz coils, we must modulate the RF signal and this is a more time consuming method of finding the resonant frequency.

Problem 3

We have the oscilloscope display the phase output of B as a function of time on the x-axis, and the output from the photo-detector on the y-axis. Surveying this data in the XY scope mode should return a Lissajous figure at resonance. We record the value of current and related frequency at each point of resonance for each isotope of Rubidium and then fit a line of best fit to find the nuclear spins and the magnetic field of the earth. The modulation of the amplitude should have no effects on the resonant frequency, hence on our data.

Appendix C

Raw Data

i [Amp]	ν [Mhz]	$T[^\circ C]$	i [Amp]	ν [Mhz]	$T[^\circ C]$
1.4043	3	30	-1.5471	3	35
1.2798	2.75	30	-1.4205	2.75	32
1.1648	2.5	35	-1.3069	2.5	36
1.0418	2.25	37	-1.1813	2.25	34
1.0174	2.197	NAN	-1.0565	2	38
0.9185	2	36	-1.0174	1.9182	NAN
0.7954	1.75	32	-0.9328	1.75	36
0.6727	1.5	37	-0.8090	1.5	35
0.5488	1.25	35	-0.6852	1.25	37
0.5153	1.1795	NAN	-0.5610	1	33
0.4246	1	35	-0.5153	0.9074	NAN
0.2994	0.75	35	-0.4366	0.75	40
0.1741	0.5	34	-0.3120	0.5	33
0.0821	0.25	36	-0.1788	0.25	32
0	0.1587	NAN	0	0.1587	NAN

Table 6: ^{85}Rb coil polarity offTable 7: ^{85}Rb coil polarity on

i [Amp]	ν [Mhz]	$T[^\circ C]$	i [Amp]	ν [Mhz]	$T[^\circ C]$
1.0174	3.2888	NAN	-1.0486	3	35
0.9117	3	30	-1.0174	2.8759	NAN
0.8299	2.75	30	-0.9662	2.75	32
0.755	2.5	35	-0.8934	2.5	36
0.6725	2.25	37	-0.8097	2.25	34
0.5895	2	36	-0.7268	2	38
0.5153	1.768	NAN	-0.6442	1.75	36
0.5067	1.75	32	-0.5614	1.5	35
0.424	1.5	37	-0.5153	1.36	NAN
0.3413	1.25	35	-0.4786	1.25	37
0.2578	1	35	-0.3956	1	33
0.1746	0.75	35	-0.3129	0.75	40
0.0899	0.5	34	-0.228	0.5	33
0.0381	0.25	36	-0.1351	0.25	32
0	0.2376	NAN	0	0.2376	NAN

Table 8: ^{87}Rb coil polarity offTable 9: ^{87}Rb coil polarity on